

# Unit Commitment Considering flexible charging of PHEVs

Yelei Wang<sup>1, a</sup>, and Xiaming Ye<sup>1, b</sup>

<sup>1</sup>College of Electrical Engineering, Zhejiang University, Hangzhou 310027, China.

<sup>a</sup>yeleiwang@gmail.com, <sup>b</sup>zjuasmn@gmail.com

**Keywords:** unit commitment (UC), vehicle-to-grid (V2G), plug-in hybrid electric vehicle (PHEV).

**Abstract.** In this paper, some boundary charging cases under unidirectional and bidirectional mode are considered to set the upper and lower bounds of the cumulative power delivery to PHEVs. A new index,  $V_{flex}$  has been proposed to quantify the flexibility provided by PHEV fleet to the power system. Empirical driving dataset is used to set up the numerical value of the boundaries. Then, based on the above idea, power constraints and energy constraints of aggregate PHEV fleet charging behavior are incorporated into the formulation of unit commitment (UC). A 10-unit system with different penetration levels of PHEVs is studied to show the benefit of system scheduling considering flexible PHEVs charging. Our study shows that a PHEV fleet used as load shifter can provide more economic benefits than used as a replacement of spinning reserve. It is also identified that the main bottleneck of flexibly using vehicle to grid technology (V2G) in unit commitment is the capacity of the batteries instead of the charging and discharging ability.

## Nomenclature

### V2G Flexibility Analysis

|                                 |   |
|---------------------------------|---|
| $E_{max}$                       | Maximum energy capacity of the battery of a PHEV.                                 |
| $E_{need}$                      | Energy needed to charge the battery to expected SOC.                              |
| $T_{max}$                       | Connected time for a single parking period.                                       |
| $T_{min}$                       | Minimum time needed to charge the battery to expected SOC.                        |
| $T_{free}$                      | Maximum time the vehicles can have no energy exchange with the grid.              |
| $VP_c^{max}$                    | Maximum charge power of the vehicle.  |
| $VP_d^{max}$                    | Maximum discharge power of the vehicle.   |
| $VP_{avg}$                      | Average charge power of the vehicle.  |
| SOC                             | State of charge of the battery. (0%~100%)   |
| $SOC_{st}$                      | Remaining SOC at the beginning of the connected time.                             |
| $SOC_{end}$                     | Expected SOC at the end of the connected time.                                    |
| $SOC_{min}$                     | Minimum SOC allowed during the V2G process.                                       |
| $SOC_{max}$                     | Maximum SOC allowed during the V2G process.                                       |
| $VP_x(t)$                       | Vehicle charge power at time $t$ in case $x$ .                                    |
| $VE_x(t) = \int_0^t VP_x(\tau)$ | Vehicle cumulative charge energy absorbed from the grid by time $t$ in case $x$ . |
| NV                              | Total number of PHEVs.  |
| $p(t)$                          | Probability of the PHEV connected to the grid at time $t$ .                       |

## Unit Commitment

### Indices

|           |                                       |
|-----------|---------------------------------------|
| $i$       | Generators $\in \{1 \dots NG\}$ .     |
| $\tau, t$ | Time intervals $\in \{1 \dots NT\}$ . |

### Binary 0/1 and integer variables at time $t$

|                 |  |
|-----------------|--|
| $I_{i,t}$       | On/Off status of unit $i$ .                  |
| $X_{i,t}^u$     | Startup status of unit $i$ .                 |
| $X_{i,t}^d$     | Shutdown status of unit $i$ .                |
| $T_{i,t}^{off}$ | Number of periods unit $i$ has been offline. |

$T_{i,t}^{on}$  Number of periods unit  $i$  has been online.

### Continuous variables of period $t$

$P_{i,t}$  Scheduled output of unit  $i$  in MW.  
 $\bar{P}_{i,t}$  Maximum available output of unit  $i$  in MW.  
 $VP_t$  Scheduled aggregate charge power of PHEV fleet in MW.  
 $\underline{VP}_t$  Minimum scheduled aggregate charge power of PHEV fleet in MW.

### Parameters

NG Total number of units.  
 NT Total number of time periods.  
 $P_i^{max}$  Maximum output of unit  $i$  in MW.  
 $P_i^{min}$  Minimum output of unit  $i$  in MW.  
 $RU_i$  Ramp-up limit of unit  $i$  in MW.  
 $RD_i$  Ramp-down limit of unit  $i$  in MW.  
 $SU_i$  Startup ramp limit of unit  $i$  in MW.  
 $SD_i$  Shutdown ramp limit of unit  $i$  in MW.  
 $UT_i$  Minimum up time of unit  $i$ .  
 $DT_i$  Minimum down time of unit  $i$ .  
 $VE_t^{max}$  Maximum cumulative energy delivery to PHEV fleet of period  $t$  in MWh.  
 $VE_t^{min}$  Minimum cumulative energy delivery to PHEV fleet of period  $t$  in MWh.  
 $VP_t^{max}$  Maximum aggregate charge power of PHEV fleet of period  $t$  in MW.  
 $VP_t^{min}$  Minimum aggregate charge power of PHEV fleet of period  $t$  in MW.  
 $D_t$  Predicted residual load demand in period  $t$  in MW.  
 $R_t$  Schedule up reserve in period  $t$  in MW.  
 $a_i, b_i, c_i$  Quadratic production cost function parameters.  
 $hc_i$  Hot startup cost of unit  $i$ .  
 $cc_i$  Cold startup cost of unit  $i$ .  
 $t_i^{cold}$  Time between hot start and cool start.

### A. Functions

$C_i^p(P_{it})$  Fuel cost function of unit  $i$  in \$.  
 $C_i^u(T_{i,t-1}^{off})$  Startup cost function of unit  $i$  in \$.  
 $C_i^d(T_{i,t-1}^{on})$  Shutdown cost function of unit  $i$  in \$.  
 $VC(VP_t, VE_t)$  Potential cost function of PHEV in \$.

### Introduction

With the development of smart grid, more and more attention has been paid on the plug-in hybrid electric vehicle(PHEV) and vehicle-to-grid(V2G) technology. The involvement of PHEVs brings both challenges and opportunities to power systems. On one hand, large number of PHEVs charge simultaneously would impact demand peaks, reduce reserve margins, and increase prices based on the simulations in [1]. On the other hand, the battery in PHEVs can be used as energy storage to mitigate the fluctuations of renewable energy. There are more than 90% of personal vehicles not in use even in traffic peak periods, making them potentially available to the grid [2].

V2G can provide competitive price when providing peak power, spinning reserves and regulation. The revenue of PHEV achievable from participating into both energy and ancillary markets are studied in [3].

In ancillary market, PHEV can provide spinning reserves and regulation power due to its fast response ability[4]. PHEV are able to provide both regulation up and regulation down services, and a

PHEV fleet can also be treated as a controllable load or even generator to charge on valley periods and discharge on peak periods.

Some papers have integrated V2G into unit commitment problem (UC-V2G). The UC formation in[5] use traffic data to give an estimation of PHEV load under different scenarios assuming PHEV only charge after their last trip. Paper [6] takes the total energy requirement of 24 hours period into account to establish PHEV fleet energy balance constraint. Paper [7] divides PHEVs into several PHEV fleet and treats each fleet as a generator.

Since household PHEVs are private properties, the grid operator has no right to make the owners to compromise to the benefits of the grid unless some economic incentives can be introduced. Any charge and discharge schedule of PHEV fleets should fulfill the energy needs of vehicle owners first. Due to the considerable size of PHEV charging demands foreseeable in the future, it will be highly beneficial if the PHEV charging schedules can be optimized and coordinated with the system operation planning i.e. UC, such that PHEVs' potentials as energy storages can be fully utilized to improve the economy and efficiency involved in system operation. Based on these considerations, a new framework for power system unit commitment scheduling incorporating the charging demands from PHEV fleets have been proposed in the paper. Most existing models for PHEVs charging scheduling recognize the stochastic nature of the problem by considering a variety of charging scenarios into the optimization model, which can be difficultly solvable due to the heavy computing loads involved. Instead, the proposed model takes into account practical driving patterns of PHEVs to formulate a feasible space of charging operations considering possible charging methods based on a novel method. Consequently, the computing efforts for the following UC optimization can be largely saved,

The paper is structured as follows. Section II analyzes the flexibility of the V2G process and proposes a new index to quantify the flexibility. Section III gives out the V2G related constraints based on the driving patterns extracted from a practical traffic dataset. Section IV describes the V2G involved unit commitment formulation. In section V, unit commitments with different penetrations of PHEV are studied. Section V concludes the paper with a summary and future scope for the research work.

## Flexibility of PHEVs Charging in Power Grids

**Introduction of the Terms.** The charging or discharging process of a single PHEV on a continuous period can be characterized by the following parameters:  $VP_c^{max}$ ,  $VP_d^{max}$ ,  $SOC_{min}$ ,  $SOC_{max}$ ,  $E_{max}$ ,  $T_{max}$ ,  $SOC_{st}$  and  $SOC_{end}$ . The first five parameters are vehicle related parameters that are fixed for a certain type of PHEV. The remaining three parameters are parking related parameters that can vary according to different parking times.  $T_{max}$  is the total V2G time, or the connected time, is a random variable in real life due to the uncertainty of PHEV owner's behavior. How to predict the parking time based on historical data and other information is important but is out of the scope of this paper. In this paper, all these parameters are assumed known when the vehicle is connected to the grid. This is not unrealistic as parameters like SOC is monitored by EV battery management system(BMS) automatically.

Some other parameters of flexible EV charging process can be determined based on the above parameters. E.g. The total energy needed in the whole parking time,  $E_{need}$ , can be calculated as,

$$E_{need} = E_{max} * (SOC_{end} - SOC_{st}) \quad (1)$$

The minimum charging time required to reach the target SOC,  $T_{min}$  is given by,

$$T_{min} = \frac{E_{need}}{VP_c^{max}} \quad (2)$$

The maximum time the vehicles have no energy exchange with the grid,  $T_{free}$  is given by,

$$T_{free} = T_{max} - T_{min} \quad (3)$$

The average charging power,  $P_{avg}$ , is given by,

$$VP_{avg} = \frac{E_{need}}{T_{max}} \quad (4)$$

**Charging Scenario Analysis.** Several charging scenarios with respect to different charging speed and power are considered for PHEVs. These methods are selected because they are relevant in formulating the boundary constraints for optimal scheduling of the charging services for a PHEV fleet, though they may not necessarily occur in the future. Therefore, only the methods which can represent boundary conditions for the charging scheduling are included. Some of the methods have been discussed in [8] but deserves further analyses herein.

**Unidirectional Mode.** In the unidirectional mode, PHEVs would not discharge to the grid. Since allowing discharging to the grid means the PHEV fleet should be treated as a generator, not just a controllable load. Additional hardware is also required to enable feeding energy back into the grid [9]. Moreover, the line loss and increased cycling wear outs on the battery would raise issues on economy and metering [10]. Therefore, the unidirectional mode is regarded most likely solution to be adopted when a large number of household PHEVs comes into service. The unidirectional mode can be further divided into several cases as follows,

#### Case u1: Fast Charging

The fast charging case considers a scenario where vehicle owners begins charging as soon as it is plugged in the grid, and stop when the SOC of the battery reaches the required amount,  $SOC_{end}$ . The vehicle will charge at its maximum charge rate,  $P_{max}$  for  $T_{min}$ , and do nothing in the remaining time  $T_{free}$ . This is the most likely case since it fulfills the charging needs in the simplest manner.

#### Case u2: Delayed Charging

The delayed charging case considers a scenario where a PHEV doesn't charge until the left parking time is just enough to fulfill the charging needs. The PHEV would do nothing for  $T_{free}$  and charge at its maximum charge rate  $P_{max}$  for  $T_{min}$ . Although this case may not happen in reality, it can be useful to establish a lower bound of energy consumption in the following studies.

#### Case u3: Uniform Charging

The uniform charging case considers a scenario where a PHEV accomplishes the charging operation given the full period of grid connection at a uniform speed, which is calculated as the required energy divided by the grid connection time, and denoted as  $VP_{avg}$ . Obviously, the small and uniform charge flow will benefit the health of the battery.

Consider a charging scenario of a PHEV with  $VP_e^{max}$  equal to 1kW. The owner would like to charge 2kWh before he picked up the vehicle 5 hours later. The charging power curve and cumulative energy delivery curve in different cases are shown in figure 1 and figure 2.

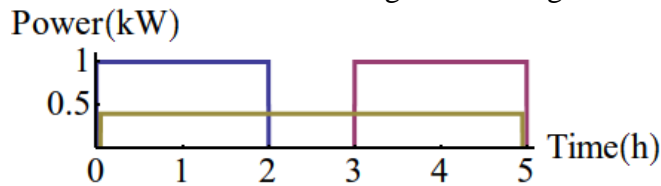


Fig. 1: Charging power curve in different cases for a single vehicle connected to the grid for a single period.

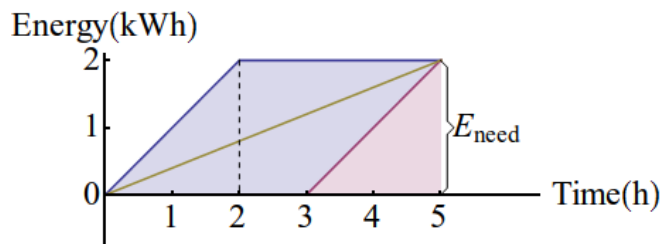


Fig. 2. Cumulative energy delivery curves in three different cases for a single vehicle connected to the grid for a single period.

From figure 1 and 2, the differences between the charging cases can be clearly seen. The curves of figure 2 all start from (0,0) and end at (5h, 2kWh), indicating that given a charging period of 5 hours, the cumulative energy delivery to the vehicle should sufficiently meet the demand of PHEV owner, no matter which charging strategy is taken. It can be found that that no matter which strategy is taken during the connection period, the cumulative energy delivery curve is always located somewhere within the parallelogram region (the region between the curves correspondence to case 1u and case 2u). Therefore case 1u and case 2u set the upper and lower bounds for the cumulative energy delivery curves.

Therefore, we can get the constraints for PHEV charging power as,

$$0 \leq VP(t) \leq VP_e^{max}, \forall t \quad (5)$$

$$\int_0^t VP_{u2}(\tau)d\tau \leq \int_0^t VP(\tau)d\tau \leq \int_0^t VP_{u1}(\tau)d\tau, \forall \tau \quad (6)$$

Equations (5) and (6) can be termed as the power and energy constraints for PHEV charging, and should be incorporated in formulating the unit commitment model later on.

**Bidirectional Mode.** The bidirectional mode allows bidirectional power flow for PHEVS, which can make full use of storage potential ability. In bidirectional mode, PHEV owners should provide an upper bound and lower bound of the SOC of the battery to avoid deep discharging and overcharging during the process. The bidirectional mode can be further divided into several cases as follows,

#### Case b1: Fast Charging

The fast charging case in bidirectional mode is somehow like the case in unidirectional mode. It would be used to set an upper bound of cumulative energy delivery in the bidirectional V2G mode. The PHEV would charge at its maximum power for as long as possible, until the SOC of the battery reaches  $SOC_{max}$ , or the remaining time left is just enough to discharge its redundant energy, whichever earlier.

#### Case b2: Delayed Charging

The delayed charging case in bidirectional mode is somehow like the case in unidirectional mode. Instead of staying idle for  $T_{free}$ , PHEV would try to discharge as deep as possible and then began its charging process. It would be used to set a lower bound of cumulative energy delivery in this mode.

#### Case b3: Uniform Charging

The uniform charging in bidirectional mode is same as that in unidirectional mode.

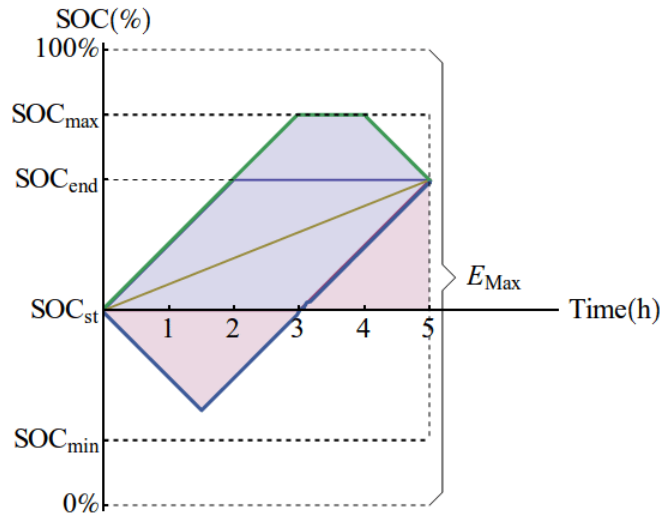


Fig. 3. SOC curves in the different cases for single vehicle connected to the grid for a single period.

Figure 3 shows that the region between lower and upper bounds in bidirectional mode is large than that in unidirectional mode, which means that there are more flexibility when taking V2G into account. The power and energy constraints in bidirectional mode are as follows.



$$VP_d^{max} \leq VP(t) \leq VP_c^{max}, \quad \forall t \quad (7)$$

$$\int_0^t VP_{b2}(\tau) d\tau \leq \int_0^t VP(\tau) d\tau \leq \int_0^t VP_{b1}(\tau) d\tau, \quad \forall \tau \quad (8)$$

**Charging Flexibility Analysis.** In order to facilitate V2G, a quantitative index of V2G flexibility should be well defined. [11] defines the flexibility as the ratio of  $T_{free}$  to  $T_{max}$ . But this definition cannot fully reflect the flexibility of charging considering many possible arrangements of charging schedules. Based on the above scenario analysis, we can define an intuitive index to better represent the flexibility of charging arrangement,  $V_{flex}$ , which is defined as the area between upper bound and lower bound of the cumulative energy delivery curve, in  $kWh \cdot h$  or  $MWh \cdot h$ .

$$V_{flex} = \int_0^{T_{max}} [VP_1(t) - VP_2(t)] dt \quad (9)$$

In unidirectional mode,  $V_{flex}$ , can be calculated easily as follows:

$$V_{flex} = T_{free} E_{need} = (T_{max} - \frac{E_{need}}{VP_{max}}) E_{need} \quad (10)$$

We can see that,  $V_{flex}$ , in unit  $kWh \cdot h$  or  $MWh \cdot h$ , can represent the ability to shift a certain amount of energy for a certain period. From (10) we can see that  $V_{flex}$  increases with the increase of  $T_{max}$  and  $VP_{max}$ , meaning that longer connection time or faster charging speed could allow for better charging flexibility. The derivative of the flexibility index with respect to  $E_{need}$  is calculated as follows:

$$\frac{dV_{flex}}{dE_{need}} = T_{max} - \frac{2E_{need}}{VP_{max}} \quad (11)$$

The derivative takes zero only when  $E_{need} = \frac{T_{max} VP_{max}}{2}$  and  $V_{flex}$  reaches its maximum value. And  $V_{flex}$  would be smaller when absolute value of  $E_{need} - \frac{T_{max} VP_{max}}{2}$  becomes large. It means that if the energy needed in the whole connected time is too large or too small, there would be not much flexibility. Consider extreme cases like  $E_{need}$  equals to zero or  $T_{max} VP_{max}$ , the PHEV has no flexibility since it must be idle or being charged at its maximum power all the time. The calculation and analysis of  $V_{flex}$  in bidirectional mode is much more complicated since the formula would include boundary parameters like  $SOC_{min}$  and  $SOC_{max}$ . It is obviously that the flexibility would increase along with the increase of gap between  $SOC_{min}$  and  $SOC_{max}$ .

### Formulation of Unit Commitment Problem Considering Flexible Charging of PHEVs

The proposed day-ahead UC formulation shown below schedules the day-ahead generation, reserve and PHEV fleet aggregate charge power on a daily basis. The objective function is as follows:

$$\text{Min } \sum_{t=1}^{NT} [\sum_{i=1}^{NG} (C_i^p(P_{i,t}) + X_{i,t}^u C_i^u(T_{i,t-1}^{off}) + X_{i,t}^d C_i^d(T_{i,t-1}^{on})) + VC(VP_t, VE_t)] \quad (12)$$

Function (12) is the total costs of the thermal unit and potential economic cost of PHEV fleet. The costs of thermal unit is composed of fuel cost for producing electric power and startup and shut down cost.

The quadratic production cost function typically used in system scheduling is as follows:

$$C_i^p(P_{i,t}) = a_i + b_i P_{i,t} + c_i P_{i,t}^2 \quad (13)$$

The startup cost is defined as a two stages step function and shut down cost is ignored here:

$$C_i^u(T_{i,t-1}^{off}) = \begin{cases} hc_i & T_{i,t-1}^{off} \leq DT_i + t_i^{cold} \\ cc_i & T_{i,t-1}^{off} > DT_i + t_i^{cold} \end{cases} \quad (14)$$

The potential economic cost including the wear-and-tear of battery and the loss of regulation up or regulation down ability due of the V2G process in energy market and so on. Social loss due to the unhappiness of PHEV owners about delay charging to the PHEV is also a potential loss. Modeling

these costs would require further research. For simplicity, we just raise a possible simple formulation of the cost function and would not use them in the following case studies.

Since the uniform charging case has low and smooth charging curve and balance the regulation up and regulation down ability at whole time. So the wear-and-tear of battery and the loss of regulation up or regulation down ability due of the V2G process can be simply modeled as  $\theta|VP_t - VP_t^{avg}|$ .

Since case u1 is the most natural charging case, the difference between cumulative energy delivery under this case and the actual cumulative energy delivery can be used as the social loss. We can model the cost as  $\mu(VE_t^{max} - VE_t)$ , which  $\mu$  is a factor in unit of \$/MWh or \$/kWh indicating the monetize of energy delivery shortage.

$$VC(VP_t, VE_t) = \theta|VP_t - VP_t^{avg}| + \mu(VE_t^{max} - VE_t) \quad (15)$$

The system constraints are as follows:

$$\sum_{i=1}^{NG} P_{it} = D_t + VP_t \quad \forall t \in \{1, 2, \dots, NT\} \quad (16)$$

$$\sum_{i=1}^{NG} \bar{P}_{it} * I_{it} \geq R_t + D_t + \underline{VP}_t, \forall t \in \{1, 2, \dots, NT\} \quad (17)$$

Constraint (16) represents the hourly power balance between the sum of scheduled generation and the sum of scheduled PHEV charge power and the expected value of the residual demand at that hour.

Constraint (17) represents the hourly system maximum available output should be no less than the sum of minimum PHEV fleet charge power, the expected value of the residual demand and predefine reserve level.

Generation limit constraints are as follows:

$$P_i^{min} * I_{i,t} \leq P_{i,t} \leq \bar{P}_{i,t} \leq P_i^{max} * I_{i,t}, \forall i \in \{1, 2, \dots, NG\}, \forall t \in \{1, 2, \dots, NT\} \quad (18)$$

$$\bar{P}_{i,t} \leq \bar{P}_{i,t-1} + RU_i * (1 - X_{i,t}^u) + SU_i * X_{i,t}^u, \forall i \in \{1, 2, \dots, NG\}, \forall t \in \{1, 2, \dots, NT\} \quad (19)$$

$$\bar{P}_{i,t} \leq \bar{P}_{i,t+1} - RD_i * (1 - X_{i,t+1}^d) - SD_i * X_{i,t+1}^d, \forall i \in \{1, 2, \dots, NG\}, \forall t \in \{1, 2, \dots, NT - 1\} \quad (20)$$

$$P_{i,t} \leq P_{i,t-1} - RD_i * (1 - X_{i,t}^d) - SD_i * X_{i,t}^d, \forall i \in \{1, 2, \dots, NG\}, \forall t \in \{1, 2, \dots, NT\} \quad (21)$$

$\bar{P}_{i,t}$  represents the available maximum output power of unit  $i$  in period  $t$  considering the ramping limit and startup and shutdown schedule. Constraints (19) represents that the maximum available output should within the ramp up or startup limit depending on the on/off status of the unit in prewise period. Constraint (20) represents that the maximum available output of unit  $i$  in period  $t$  should also take the shutdown schedule in future period into consideration to avoid violation of the schedule.

The minimum up and down time limits are as follows:

$$T_{i,t-1}^{on} \geq X_{i,t}^d * UT_i, \forall i \in \{1, 2, \dots, NG\}, \forall t \in \{1, 2, \dots, NT\} \quad (22)$$

$$T_{i,t-1}^{off} \geq X_{i,t}^u * DT_i, \forall i \in \{1, 2, \dots, NG\}, \forall t \in \{1, 2, \dots, NT\} \quad (23)$$

Constraints (22) and (23) represent the minimum up and down time limits of thermal units.

The V2G Constraints are as follows:

$$VP_t^{min} \leq VP_t \leq VP_t^{max}, \quad \forall t \in \{1, 2, \dots, NT\} \quad (24)$$

$$VE_t^{min} \leq \sum_{\tau=1}^t VP_{\tau} * 1h \leq VE_t^{max}, \forall t \in \{1, 2, \dots, NT\} \quad (25)$$

$$\underline{VP}_t = \max \left( VP_{min}, \frac{VE_t^{min}}{1h} - \sum_{\tau=1}^{t-1} VP_{\tau} \right), \forall t \in \{1, 2, \dots, NT\} \quad (26)$$

Constraints (24)-(26) are the power and energy constraints for the PHEV fleet. Constraint (25) represents that the minimum charge power should fulfill the energy requirement of PHEV fleet. Since VP is power unit in MW and VE is energy unit in MWh and cannot be compared directly, a time unit is introduced here to make them comparable.

**Mixed Integer Linear Formulation.** In order to guarantee the convergence to the optimal solution while enabling the flexibility of the developed framework, the problem should be formatted as a MIP problem. Most of the linearization technique needed can be found in [12]. Some other part would be handled as follows:

The ordinary representation of the startup status is  $X_{i,t}^u = I_{i,t} * (1 - I_{i,t-1})$ , which introduce nonlinear constraints. It can be replaced by three linear constraints as follows:

$$X_{i,t}^u \leq I_{i,t}, \forall t \in \{1, 2, \dots, NT\} \quad (27)$$

$$X_{i,t}^u \leq 1 - I_{i,t-1}, \forall t \in \{1, 2, \dots, NT\} \quad (28)$$

$$X_{i,t}^u \geq 1 + I_{i,t} - I_{i,t-1}, \forall t \in \{1, 2, \dots, NT\} \quad (29)$$

The constraints about shutdown status are similar. In actual optimization programing,  $X_{i,t}^u$  and  $X_{i,t}^d$  don't need to be specified as binary variable to improve computational efficiency.

### Constraints of PHEV Changing Based on Practical Driving Patterns

**Dataset Specification.** Here we use TU data (Danish National Transport Survey) as the data source for driving pattern analysis and establishing the V2G related constraints. The TU data are interview data collect daily for more than 10 years. More than 100,000 household interviewees are asked to provide their driving profile on a particular day, including the start time, end time and distance traveled of each trip, the personal information like sex, family size, and home location and so on. Some interesting statistics from this dataset has been studied in [2].

**Basic Assumption.** Since these driving data are collected from conventional vehicle owners, there might be some inconsistency with actual PHEV driving pattern and PHEV might not be likely to plug in the grid wherever it parked. Assuming PHEV drivers would keep their driving behavior and are able to stay connected with the grid anywhere still makes a good approximation of the future stage where PHEVs are widely deployed with well-established charging infrastructures in urban area. It is also assumed that critical parameters governing PHEVs charging services are as those listed in Table 1.

Table 1 PHEV Parameters for V2G Study

| Information             | Value of Parameter |
|-------------------------|--------------------|
| Maximum allow SOC       | 85%                |
| Minimum allow SOC       | 10%                |
| Energy capacity         | 15kWh              |
| Maximum charge power    | 2kW                |
| Maximum discharge power | 1.2kW              |
| Energy used per km      | 150Wh/km           |

In our case study alter on, for each PHEV, it is assumed that it would charge to  $SOC_{max}$  before the departure time of the first trip of the day, and it would try to charge as much as possible in each parking period.

**Charging Power Constraints.** The power constraints of the PHEV fleet depend on the number of PHEV connected to the grid and maximum charge and discharge power limits of each PHEV. From the dataset it has been analyzed that that the driving patterns from Monday to Thursday are more or less the same with only small differences. We can generate the time series that private cars are not on the road during weekdays to help formulate the charging power constraints considering a PHEV fleet.



Table 2 Connected vehicles per 10,000 PHEVs in weekdays (excluding Friday)

|             |      |      |      |      |      |      |
|-------------|------|------|------|------|------|------|
| Hour Number | 1    | 2    | 3    | 4    | 5    | 6    |
|             | 9984 | 9993 | 9996 | 9994 | 9982 | 9911 |
| Hour Number | 7    | 8    | 9    | 10   | 11   | 12   |
|             | 9661 | 9361 | 9563 | 9735 | 9728 | 9746 |
| Hour Number | 13   | 14   | 15   | 16   | 17   | 18   |
|             | 9733 | 9723 | 9636 | 9403 | 9355 | 9533 |
| Hour Number | 19   | 20   | 21   | 22   | 23   | 24   |
|             | 9687 | 9806 | 9869 | 9866 | 9890 | 9941 |

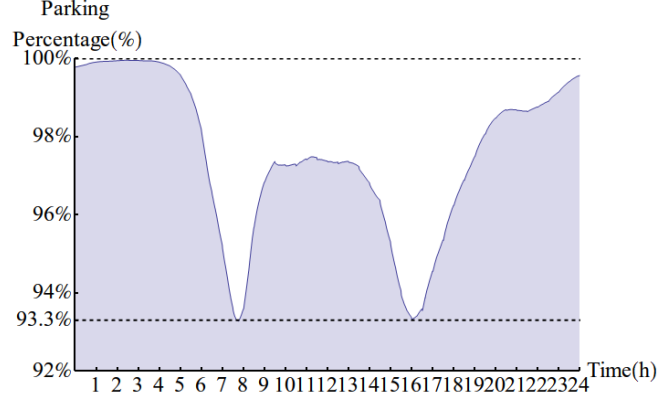


Fig. 4. Probability that household cars are not in use for transportation during weekdays.

Figure. 4 shows the percentage of parking vehicles over the total in weekdays. Though there are two valleys due to the peak hours, the fraction of parking vehicles is still no less than 93%. The hourly average numbers of parking vehicles per 10,000 vehicles are listed in Table 2. Given the total number of household PHEVs within a fleet, NV, the charging power constraints can be expressed as follows:

$$VP^{max}(t) = p(t) * NV * P_{c,avg}^{max} \quad (30)$$

$$VP^{min}(t) = \begin{cases} 0, & \text{unidirectional mode} \\ -p(t) * NV * P_{d,avg}^{max}, & \text{bidirectional mode} \end{cases} \quad (31)$$

**Charging Energy Constraint.** Base on the assumption that PHEV would try to charge as much energy as possible, the charging power curve in each cases in Section II can be calculated. For the overnight parking (parking time contains 24:00), it would be separated by 24:00 into two parking periods to set boundary condition of the 24 hour cumulative power delivery curve.

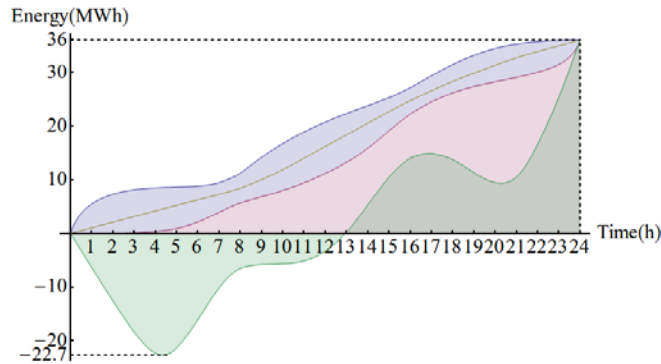


Fig. 5. The cumulative energy delivery in each case on weekdays per 10,000 PHEVs

Form figure 5 we can see that the aggregate energy requirement of 10,000 PHEVs in a single weekday is about 36 MWh, which means that each PHEV would have 24km daily electric mileage in average on weekdays. The uniform charging is just in the middle between the upper and lower bounds of the unidirectional mode. And we can see that the flexibility is smaller during the commute periods

due to the travel needs. In bidirectional mode, the upper bound is the same as the one under unidirectional mode since we assume that PHEV would try to absorb as much energy as possible during the V2G process. It can be seen that the lower bound of bidirectional mode is more lower than that in unidirectional mode, which means there would be much more flexibility in bidirectional mode. The hourly lower and upper bounds for cumulative energy delivery are listed in Table 3.

Table 3. Cumulative energy delivery to PHEV fleet in different charging cases per 10,000 PHEVs in weekdays (excluding Friday)

| Hour (h) | Case u1/b1 (MWh) | Case u2 (MWh) | Case b2 (MWh) | Case u3/b3 (MWh) |
|----------|------------------|---------------|---------------|------------------|
| 1        | 5.4845           | 0.0152        | -6.3557       | 1.0485           |
| 2        | 7.2827           | 0.0401        | -12.5947      | 2.0979           |
| 3        | 8.1353           | 0.1160        | -18.3921      | 3.1468           |
| 4        | 8.4794           | 0.3467        | -22.3290      | 4.1973           |
| 5        | 8.6358           | 0.9289        | -21.3538      | 5.2426           |
| 6        | 8.8077           | 2.1260        | -16.1235      | 6.2690           |
| 7        | 9.4508           | 3.9408        | -10.1845      | 7.2780           |
| 8        | 11.2356          | 5.6889        | -6.5174       | 8.4346           |
| 9        | 14.1672          | 6.8428        | -5.7802       | 10.0238          |
| 10       | 16.7362          | 8.0401        | -5.6200       | 11.9068          |
| 11       | 18.9008          | 9.4488        | -5.1103       | 14.0263          |
| 12       | 20.7366          | 11.2052       | -3.2862       | 16.2257          |
| 13       | 22.3500          | 13.2709       | 0.2770        | 18.3822          |
| 14       | 23.8046          | 15.9146       | 5.3402        | 20.5598          |
| 15       | 25.3173          | 19.1597       | 10.5124       | 22.7319          |
| 16       | 27.1645          | 22.2739       | 14.0476       | 24.7755          |
| 17       | 29.3839          | 24.5393       | 14.9039       | 26.6411          |
| 18       | 31.4623          | 26.2152       | 13.7805       | 28.3466          |
| 19       | 33.1846          | 27.4079       | 11.3873       | 29.8955          |
| 20       | 34.4901          | 28.2720       | 9.4897        | 31.3664          |
| 21       | 35.2940          | 29.0917       | 10.5389       | 32.7429          |
| 22       | 35.7409          | 30.0619       | 16.5877       | 33.9397          |
| 23       | 35.9785          | 31.4913       | 25.3815       | 35.0109          |
| 24       | 36.0494          | 36.0494       | 36.0494       | 36.0494          |

## Case Studies

The proposed formulation has been applied to solve the ten-unit of [13]. The load demand and system parameters are listed in Tables A~C in appendix of [13]. The system reserve of each time period is set to be 10% of the total demand.

The penetration of V2G is defined as the ratio of the aggregate energy consumed by PHEV fleet to the total energy consumed by whole society on daily basis. From the load demand data in Table A, it shows that the total energy consumption in 24 hours is 27,100 MWh. So, 1% penetration of V2G means PHEV fleet draw 271MWh energy from the grid in 24 hours. That is about 75,000 PHEVs in total.

In order to show the impacts of different penetrations of V2G, the demand scales down and number of PHEVs scales up to make the daily total energy consumption unchanged while reserve maintaining the same level.

The model has been implemented on a PC with two processors at 2.13 GHz and 2GB of RAM memory using Gurobi 5.0 to solve this MILP-UC problem. Solver has been called from AIMMS. All results would be expressed in US Dollar (\$).

The original UC problem is used as base-line case. The daily cost is \$576372.358 and the commitment schedule is listed in Table 4.

Table 4: UC without V2G involved

| Daily Cost = \$576372.358 |   |
|---------------------------|---|
| Unit                      | Hours(1-24)                                     |
| 1                         | 1 |
| 2                         | 1 |
| 3                         | 0 0 0 0 0 1 1 1 1 1 1 1 1 1 1 1 1 1 1 1 1 1 1 0 |
| 4                         | 0 0 0 1 0 |
| 5                         | 0 1 0 |
| 6                         | 0 0 0 0 0 0 0 1 1 1 1 1 1 1 1 0 0 0 1 1 1 1 1 0 |
| 7                         | 0 0 0 0 0 0 0 0 1 1 1 1 1 1 0 0 0 0 1 1 1 0 0 0 |
| 8                         | 0 0 0 0 0 0 0 0 1 1 1 1 1 1 0 0 0 0 1 1 1 0 0 0 |
| 9                         | 0 0 0 0 0 0 0 0 0 1 1 1 1 0 0 0 0 0 0 0 0 0 0 0 |
| 10                        | 0 0 0 0 0 0 0 0 0 0 1 1 1 0 0 0 0 0 0 0 0 0 0 0 |

**Unidirectional Cases.**By ignoring the potential economic loss of PHEV fleet and set the penetration of V2G to 10%. The result of the Unit commit problem is \$538106.652. Compare to base line case, we can see that total cost has been reduced by \$21676.1.

Table 5: UC with unidirectional V2G involved (10% penetration)

| Daily Cost = \$538106.652 |   |
|---------------------------|---|
| Unit                      | Hours(1-24)                                     |
| 1                         | 1 |
| 2                         | 1 |
| 3                         | 0 0 0 0 0 0 0 1 1 1 1 1 1 1 1 1 1 1 1 1 1 1 1 0 |
| 4                         | 0 0 0 1 0 |
| 5                         | 0 0 0 1 0 |
| 6                         | 0 0 0 0 0 0 0 0 1 1 1 1 1 1 0 0 0 0 1 1 1 1 0 0 |
| 7                         | 0 0 0 0 0 0 0 0 0 1 1 1 1 0 0 0 0 0 0 0 0 0 0 0 |
| 8                         | 0 0 0 0 0 0 0 0 0 0 0 1 0 0 0 0 0 0 0 0 0 0 0 0 |
| 9                         | 0 |
| 10                        | 0 |

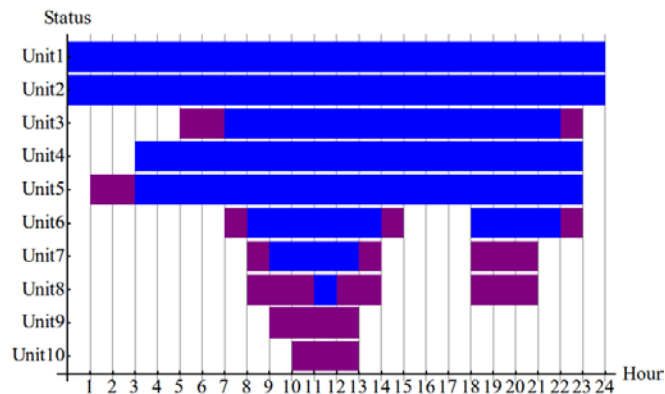


Fig 6: Difference between the schedules of original UC and UC with unidirectional V2G involved (10% penetration).

From figure 6 we can see that, with the involvement of V2G, some expensive units don't need not to be committed in the new schedule.

The reduction of cost is composed by two parts, the load-shift part and the reserve part. The load-shift part is the cost saved by shifting the load from peak period to valley period. The reserve part is the cost saved by replacing expensive thermal spinning reserve to the reserve provide by PHEV fleet.

In order to quantify the value of these two parts of cost saving, we replace  $VP_t$  by  $VP_t$  in constraint (6) and solve the unit-commitment problem again. Then the result of UC with PHEV fleet used only as load-shifter can be acquired and the difference between the result of this UC problem and prewise UC problem is the part of cost saving by reserve replacement. Table 6 shows the cost saving under different penetrations of V2G.

Table 6: Cost saving under different penetrations of unidirectional V2G

| Penetration | Total Saving (\$) | Load shift part (\$) | Reserve part (\$) |
|-------------|-------------------|----------------------|-------------------|
| 1%          | 1520.4            | 1362.5               | 158.0             |
| 2%          | 3925.6            | 3637.9               | 287.6             |
| 3%          | 8580.9            | 8147.1               | 433.8             |
| 4%          | 10179.3           | 9452.6               | 726.7             |
| 5%          | 11298.1           | 9793.9               | 1504.2            |
| 6%          | 13495.5           | 11729.8              | 1765.7            |
| 7%          | 16035.7           | 13326.9              | 2708.8            |
| 8%          | 17629.3           | 14113.3              | 3516.0            |
| 9%          | 19310.4           | 15775.8              | 3534.6            |
| 10%         | 21676.7           | 17229.3              | 4447.4            |

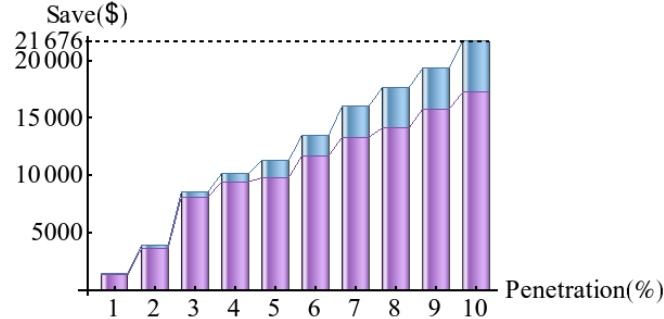


Fig. 7: The cost saving under different penetrations of unidirectional V2G

From figure 7 we can see that, the saving by load-shift can save more cost than that by reserve replacement.

Table 7: Scheduled aggregate charge power of PHEV fleet in unidirectional mode (10% penetration)

| Hour       | 1      | 2      | 3      | 4      | 5      | 6      |
|------------|--------|--------|--------|--------|--------|--------|
| Demand(MW) | 185.00 | 189.42 | 99.42  | 54.42  | 79.42  | 54.42  |
| Hour       | 7      | 8      | 9      | 10     | 11     | 12     |
| Demand(MW) | 48.35  | 115.80 | 115.80 | 90.80  | 45.80  | 10.80  |
| Hour       | 13     | 14     | 15     | 16     | 17     | 18     |
| Demand(MW) | 90.80  | 128.05 | 138.05 | 248.94 | 293.94 | 208.94 |
| Hour       | 19     | 20     | 21     | 22     | 23     | 24     |
| Demand(MW) | 198.94 | 0.00   | 3.94   | 73.94  | 125.00 | 110.00 |

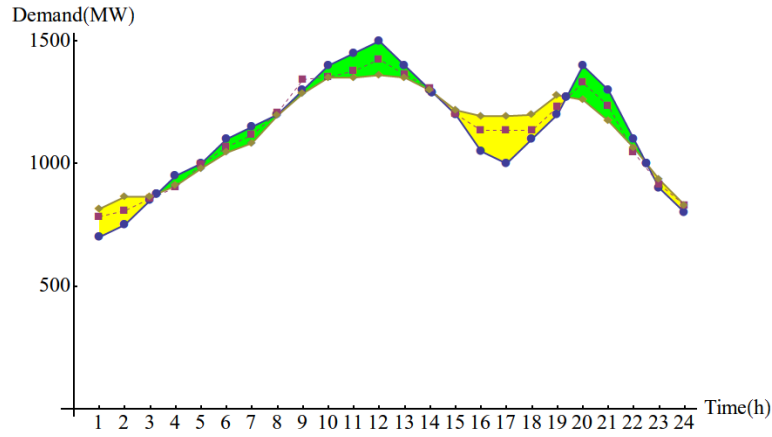


Fig. 8: Total load demand under different penetrations of unidirectional V2G.

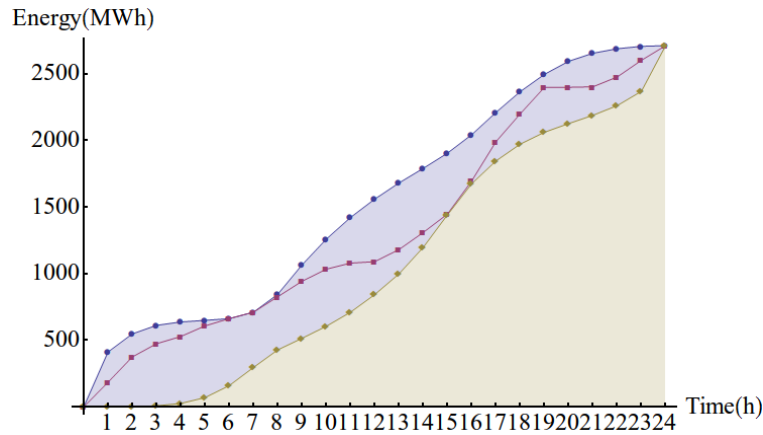


Fig. 9: Cumulative energy delivery to PHEV fleet in unidirectional mode (10% penetration)

Table 7 shows the scheduled aggregate charge power of PHEV fleet, the charging power is far lower than the maximum charging ability (The maximum charging ability with 10% penetration of V2G is about 1500MW). It means that charging power ability of PHEV fleet is enough to the whole power system with this level of penetration. Figure 8 show that the PHEV fleet shifts the load from peak period (the green part) to the valley period (the yellow part). Figure 9 shows that the cumulative energy delivery curve reaches the upper bound of the energy constraint in 6a.m. and 7a.m., and reaches the lower bound of the energy constraint in 3p.m. and 4p.m. It shows that the main bottleneck preventing PHEV fleet from shifting more energy between peak and valley periods is the energy constraint. In the valley periods in evening, PHEV fleet is scheduled to absorb more energy and the bottleneck is the capacity of batteries. In peak periods at noon, PHEV fleet is scheduled to absorb less energy but it must meet the energy requirement before PHEV owners pickup their car for commuting.

**Bidirectional Mode.** In bidirectional mode, the saving cost would be more that in same penetration in unidirectional mode, since the allowance of discharge provides more reserve and more ability to shift more energy. By ignoring the potential economic loss of PHEV fleet and set the penetration of V2G to 10%. The result of the unit commit problem is \$541306.2932. Compare to base line case, we can see that total cost has been reduced by \$35066.1.



Table 8: UC with bidirectional V2G involved (10% penetration)

| Daily Cost=\$541306.293 |   |
|-------------------------|---|
| Unit                    | Hours(1-24)                                       |
| 1                       | 1   |
| 2                       | 1   |
| 3                       | 0 0 0 0 0 0 1 1 1 1 1 1 1 1 1 1 1 1 1 1 1 1 1 1   |
| 4                       | 0 0 0 1   |
| 5                       | 0 0 0 0 0 0 0 0 1 1 1 1 1 1 1 1 1 0 0 0 0 0 0 0 0 |
| 6                       | 0 |
| 7                       | 0 |
| 8                       | 0 |
| 9                       | 0 |
| 10                      | 0 |

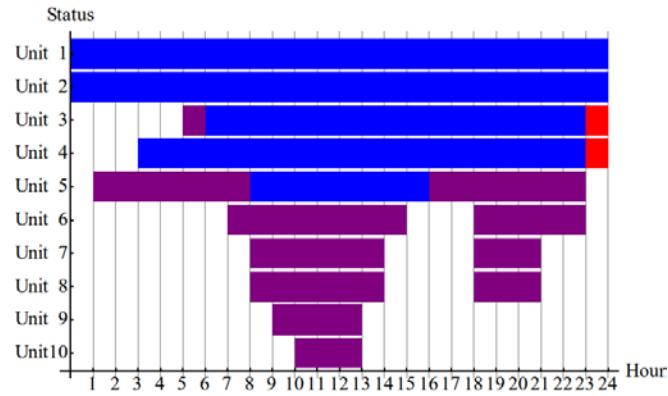


Fig 10: Difference between the schedules of original UC and UC with 10% penetration of bidirectional V2G involved.

Table 9: Cost saving under different penetrations of bidirectional V2G

| Penetration | Total Saving (\$) | Load shift part (\$) | Reserve part (\$) |
|-------------|-------------------|----------------------|-------------------|
| 1%          | 15408.6           | 10101.7              | 5306.9            |
| 2%          | 23937.9           | 15136.4              | 8801.5            |
| 3%          | 29566.7           | 19515.6              | 10051.0           |
| 4%          | 32818.1           | 20706.1              | 12111.9           |
| 5%          | 33670.7           | 21385.4              | 12285.3           |
| 6%          | 33809.9           | 22076.2              | 11733.7           |
| 7%          | 34415.3           | 23762.0              | 10653.2           |
| 8%          | 34980.8           | 24004.1              | 10976.7           |
| 9%          | 35023.8           | 24256.9              | 10766.8           |
| 10%         | 35066.1           | 24539.2              | 10526.9           |

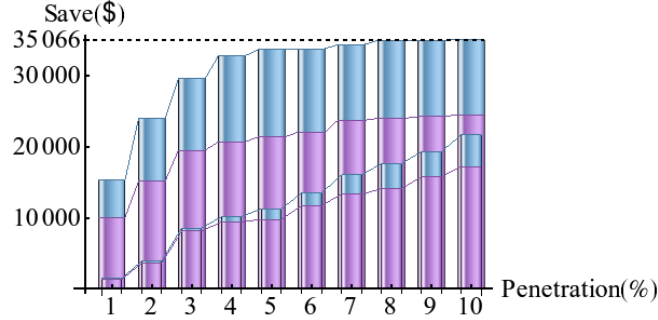


Fig 11: Cost saving under different penetrations of bidirectional V2G comparing to that with unidirectional V2G.

From figure 11 we can see that, the cost saving with bidirectional V2G is much more than that with unidirectional V2G. The growing rate of cost saving is much slower when the penetration of bidirectional V2G became large.

Table 10: Scheduled aggregate charge power of PHEV fleet in bidirectional mode (10% penetration)

| Hour       | 1      | 2      | 3      | 4      | 5      | 6      |
|------------|--------|--------|--------|--------|--------|--------|
| Demand(MW) | 185.00 | 200.00 | 121.78 | 51.78  | 76.78  | 26.78  |
| Hour       | 7      | 8      | 9      | 10     | 11     | 12     |
| Demand(MW) | 25.00  | 50.00  | 25.00  | -5.00  | 8.22   | -36.78 |
| Hour       | 13     | 14     | 15     | 16     | 17     | 18     |
| Demand(MW) | 53.22  | 143.22 | 175.00 | 250.00 | 270.00 | 180.00 |
| Hour       | 19     | 20     | 21     | 22     | 23     | 24     |
| Demand(MW) | 90.00  | -90.00 | 0.00   | 180.00 | 360.00 | 370.00 |

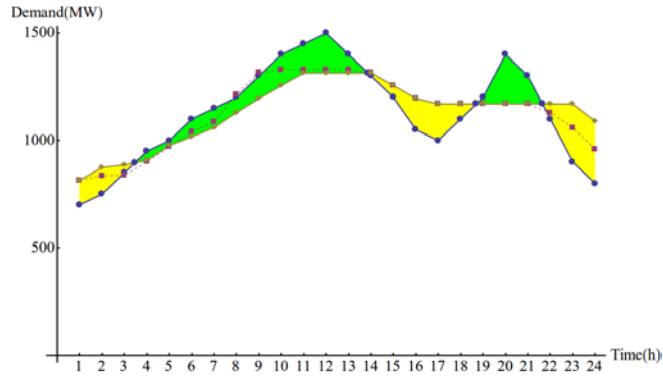


Fig. 12: Total load demand under different penetrations of bidirectional V2G.

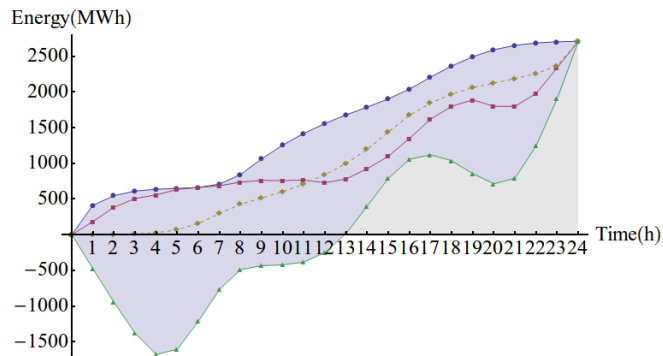


Fig. 13: Cumulative energy delivery to PHEV fleet in bidirectional mode (10% penetration)

Table 10 shows the scheduled aggregate charge power of PHEV fleet, the charging power is still far lower than the maximum charging ability (The maximum discharging ability with 10% penetration of V2G is about 900MW). It means that charging power ability of PHEV fleet is enough to the whole power system with this level of penetration. Figure 12 show that the PHEV fleet shifts the load from peak period (the green part) to the valley period (the yellow part). And we can see that the energy shifted by PHEV fleet is more than that in unidirectional mode. Figure 13 show that the curve never reaches the lower bound of the energy requirement since lower bound is much lower now. It means that the energy requirement for the night commuting is fulfilled by some other parking PHEVs.

## Conclusion and Future Work

From the above study we can conclude that V2G technology can bring much benefit to the power system. In UC problem in energy market, bidirectional V2G can save more money than unidirectional V2G. Our study shows that PHEV fleet used as load shifter can save more money than be used as a replacement of spinning reserve. The figure about cumulative energy delivery states that the capacity of batteries on PHEV is the main bottleneck of V2G.

V2G can play an important role in ancillary market and may earn more profile profit than energy market. But it is hard to model the profit in ancillary market into the formulation of UC problem. In the previse formulation, we try to establish a link between energy market and ancillary market by introducing a simple penalty function into the cost function. In future work, a more accurate penalty function would be set up to optimize the charging behavior of PHEV fleet both in energy market and ancillary market.

In this paper, we only give the best feasible schedule of aggregate charging power of the whole PHEV fleet. But in real world, the charging power needs to be disaggregated to each charging station or even each charging pole and it might be a difficult job. A practical way might be introduce a price single as incentive and how to determine the price at each time to narrow the difference between real aggregate charging power and scheduled aggregate charging power needed further study.

## References

- [1] S. W. Hadley and A. A. Tsvetkova, Potential Impacts of Plug-in Hybrid Electric Vehicles on Regional Power Generation, *The Electricity Journal*. 22(2009) 56-68
- [2] W. Qiuwei, A. H. Nielsen, D. J. stergaard, C. Seung Tae, F. Marra, C. Yu, Tr, E, and C. holt, Driving Pattern Analysis for Electric Vehicle (EV) Grid Integration Study, *Innovative Smart Grid Technologies Conference Europe (ISGT Europe)*, 2010 IEEE PES, (2010) 1-6.
- [3] W. Kempton and J. Tomić, Vehicle-to-grid power fundamentals: Calculating capacity and net revenue, *Journal of Power Sources*. 144(2005) 268-279.
- [4] E. Sortomme and M. A. El-Sharkawi, Optimal Scheduling of Vehicle-to-Grid Energy and Ancillary Services, *IEEE Transactions on Smart Grid*, 3(2015) 351-359.
- [5] L. Cong, W. Jianhui, A. Botterud, Z. Yan, and A. Vyas, Assessment of Impacts of PHEV Charging Patterns on Wind-Thermal Scheduling by Stochastic Unit Commitment, *IEEE Transactions on Smart Grid*, 3(2012) 675-683.
- [6] A. Y. Saber and G. K. Venayagamoorthy, Unit commitment with vehicle-to-Grid using particle swarm optimization, in *PowerTech, 2009 IEEE Bucharest*, (2009) 1-8.
- [7] M. E. Khodayar, L. Wu, and M. Shahidehpour, Hourly Coordination of Electric Vehicle Operation and Volatile Wind Power Generation in SCUC, *IEEE Transactions on Smart Grid*, (2012). (online access)

- [8] P. K. D. P, and M. T, Costs and emissions associated with plug-in hybrid electric vehicle charging in the Xcel energy Colorado, service territory [EB/OL]. National Renewable Energy Laboratory Technical Report (2007).
- [9] E. Sortomme and M. A. El-Sharkawi, Optimal Charging Strategies for Unidirectional Vehicle-to-Grid, IEEE Transactions on Smart Grid, 2(2011) 131-138.
- [10] S. B. Peterson, J. Apt, and J. F. Whitacre, Lithium-ion battery cell degradation resulting from realistic vehicle and vehicle-to-grid utilization, Journal of Power Sources, 195(2010), 2385-2392.
- [11] P. B. Nørgård and L. Christensen, Estimated impact of the uncertainties in the driving patterns on the power system flexibility provided by electrical vehicles, 2009. Information on [http://orbit.dtu.dk/en/publications/estimated-impact-of-the-uncertainties-in-the-driving-patterns-on-the-power-system-flexibility-provided-by-electrical-vehicles\(cfb6d52a-5041-4998-a836-b00843f1890b\)/export.html](http://orbit.dtu.dk/en/publications/estimated-impact-of-the-uncertainties-in-the-driving-patterns-on-the-power-system-flexibility-provided-by-electrical-vehicles(cfb6d52a-5041-4998-a836-b00843f1890b)/export.html).
- [12] M. Carrion and J. M. Arroyo, A computationally efficient mixed-integer linear formulation for the thermal unit commitment problem, IEEE Transactions on Power Systems, 21(2006) 1371-1378.
- [13] S. A. Kazarlis, A. G. Bakirtzis, and V. Petridis, A genetic algorithm solution to the unit commitment problem, IEEE Transactions on Power Systems, 11(1996) 83-92.